Fragment Reconstitution of a Small Protein: Folding Energetics of the Reconstituted Immunoglobulin Binding Domain B1 of Streptococcal Protein G[†]

Shinya Honda,*[,‡] Naohiro Kobayashi,[§] Eisuke Munekata,[§] and Hatsuho Uedaira[‡,||]

National Institute of Bioscience and Human Technology, Tsukuba, Ibaraki 305-8566, Japan, Institute of Applied Biochemistry, University of Tsukuba, Tsukuba, Ibaraki 305-8572, Japan, and Tsukuba Life Science Center, RIKEN, Tsukuba, Ibaraki 305-0074, Japan

Received September 21, 1998

ABSTRACT: To elucidate early stages in protein folding, we have adopted a fragment reconstitution method for small proteins. This approach is expected to provide nuclei for protein folding and to allow us to investigate folding mechanisms. In previous work [Kobayashi, N., et al. (1995) *FEBS Lett. 366*, 99−103.] we demonstrated the association of two complementary fragments, derived from the immunoglobulin G-binding domain B1 of streptococcal Protein G, and showed the structural similarity between the reconstituted domain and the uncleaved wild-type domain. In this work we have further characterized the reconstituted domain as well as the uncleaved domain thermodynamically by means of differential scanning calorimetry (DSC) and circular dichroism (CD) measurements. Although composed of short peptide fragments not linked by covalent bonds, the reconstituted domain showed a typical folding/unfolding curve in both DSC and CD melting measurements and behaved like a globular protein. The domain was not very stable, and the small value of the Gibbs free energy corresponded to the class of the weakest protein−protein binding systems. The denaturation temperature of 0.78 mM solution was 313 K at pH 5.9 as measured by DSC, which was more than 40 degrees lower than the uncleaved domain. This apparent instability was primarily caused by entropic disadvantage attributed to a bimolecular reaction. The temperature dependence of the enthalpy change from the folded to the unfolded state was almost identical for the reconstituted domain and the uncleaved one. This indicates that most of the noncovalent intramolecular interactions stabilizing the native structure, such as hydrogen bonding and hydrophobic interactions, are regenerated in the reconstituted domain. By comparing the equilibrium constants of the reconstituted and uncleaved domains, we determined the effective concentration to be approximately 6 M at 298 K. Structure-based estimation of the thermodynamic properties from the values of accessible surface areas showed that approximately 35% of the total heat capacity change and approximately 25% of the total enthalpy change can be attributed to the interchain interaction at 298 K. Furthermore, the folding/unfolding equilibrium of β-hairpin structure of the fragment 41−56 alone was also characterized. These analyses allow us to envision the microdomain folding mechanism of the Protein G B1 domain, in which segment 41−56 first forms a stable β-hairpin structure and then collides with segment 1−40, followed by spontaneous folding of the whole molecule.

As often phrased in terms of the Levinthal paradox (*1*), there is a mystery in that the process of protein folding proceeds too quickly to reduce an astronomical number of conformational degrees of freedom, present in the unfolded state, to a limited number in the folded state. It is generally accepted that proteins must fold through a particular pathway or set of pathways (*2*), or via some slope on a funnel-like energy landscape (*3*−*5*). However, it is not easy to predict the pathway of an individual protein because the mechanism of protein folding is so complicated. Since the relatively slow processes in protein folding, corresponding to disulfide bond formation, proline isomerization, or multidomain formation, have been extensively examined (*6*−*8*), many investigations have focused on the fast processes that occur in the early stages of protein folding. To study the fast processes in the early stages, it is essential to choose simple proteins that lack disulfide bonds and prolines, because such proteins are free of the complications caused by above slow processes.

Immunoglobulin G-binding domain B1 of streptococcal protein G (PGB1)[1] is a small protein consisting of 56 amino acid residues. It is composed of a stable single domain and has neither cysteins nor prolines. In addition, the physicochemical properties of PGB1 have been well investigated. Its tertiary structure was determined by NMR spectroscopy

[†] This work was supported by a grant from the Agency of Industrial Science and Technology, MITI, Japan.

* To whom correspondence should be addressed. E-mail: honda@nibh.go.jp. Fax: +81-298-54-6194.

[‡] National Institute of Bioscience and Human Technology.

[§] University of Tsukuba.

[||] RIKEN.

10.1021/bi982271g CCC: $18.00
Published on Web 01/12/1999

(*9*) and X-ray crystallography (*10*, *11*). The thermodynamic properties were analyzed by calorimetric methods (*12*) and hydrogen−deuterium exchange (*13*, *14*). The kinetic folding behavior was measured by the stopped-flow pH jump method (*15*), the quenched flow plus deuterium−hydrogen exchange technique (*16*), and the stopped-flow fluorescence method (*17*). Fragment conformations in aqueous or aqueous/trifluoroethanol solutions were characterized by NMR spectroscopy and circular dichroism (CD) (*18*−*21*). Thus, PGB1 can be considered to be an ideal sample for elucidating the early stages in protein folding.

Generally, a small protein folds very rapidly. Therefore, many difficulties arise in real-time observations of the folding of a small protein. In fact, the folding of PGB1 at neutral pH takes less than 2 ms (*15*, *17*). To avoid such difficulties we adopted a "fragment reconstitution" approach in which we first cleaved a protein and made several pairs of peptide fragments. Then we determined their structural properties at equilibrium. This produced a "microdomain" (*22*), which was stabilized by a local interaction among neighboring residues and was thus a candidate for being a nucleus or an intermediate in the folding process. Next we examined the specific association of a pair of fragments. This revealed a nonlocal interaction between microdomains. Using the above approach we were able to visualize protein folding as if time had stopped. In a previous paper (*23*) we investigated the structure of the reconstituted PGB1 domain, composed of the two complementary fragments [i.e., PGB1(1−40) and PGB1(41−56)], by NMR spectroscopy and CD measurements. The results demonstrated that the domain has a nativelike secondary structure and that part of the domain folds to the same tertiary structure as for the uncleaved wild-type domain. However, the quantitative degree of reconstitution was not investigated.

In this work we have carried out the thermodynamic analysis of the reconstituted domain composed of the two fragments [PGB1(1−40) and PGB1(41−56)], as well as the uncleaved wild-type domain. Initially, we have checked whether the reconstituted domain shows thermal denaturation like globular proteins. After confirming the detectable transition, we have performed DSC and CD melting measurements of the reconstituted domain and then analyzed them using equations that we developed to determine thermodynamic properties of the domain. The properties were compared with that of ordinary protein−protein binding systems to understand the stability of the reconstituted domain. Finally, on the basis of the thermodynamic comparison with the uncleaved domain, we have evaluated the folding energetics of PGB1 and discussed its folding mechanism.

MATERIALS AND METHODS

Proteins. Immunoglobulin G-binding domain B1 of streptococcal Protein G (PGB1) and its fragments [PGB1(1−40) and PGB1(41−56)] were synthesized by Fmoc strategy and purified by reverse-phase HPLC. The sequences of the synthesized proteins were confirmed by amino acid analysis, amino acid sequencing, and mass spectroscopy, as previously described in detail (*23*).

CD Spectrum and CD Melting Measurements. A lyophilized sample of PGB1 or its fragment was dissolved in either 50 mM phosphate buffer or 100 mM β,β'-dimethylglutaric acid (DMG) buffer solution. DMG buffer was selected in order to cancel out the heat of ionization of carboxylate groups during unfolding. The concentrations of the samples were determined by their theoretical absorbances at 280 nm [ϵ_{280} = 2560, 6970, and 9530 for PGB1(1−40), PGB1(40−56), and PGB1(1−56), respectively], calculated from the standard values of Trp and Tyr (*24*). Fragment reconstitution of PGB1(1−40) with PGB1(40−56) was carried out with vortex mixing of the two fragments in an equimolar ratio. Before measurements, the sample solutions were dialyzed against a hundred-time volume buffer for at least 8 h at 277 K.

CD spectra were measured by a Jasco J-600 spectropolarimeter (Tokyo, Japan) and represented as the units of the molecular ellipticity per mole of protein. Measurement conditions were as described previously (*25*, *26*). CD melting measurements were carried out with our original system which consisted of a Jasco J-600 spectropolarimeter, Haake circulator F3 (Germany), Chino digital program controller Model KP (Tokyo, Japan), and handmade software (*27*). By using this system, we collected values of both molecular ellipticity and temperature of the sample simultaneously every second as digital data. The heating and cooling rates were fixed at 0.5 K/min in all measurements.

DSC Measurements. Sample solutions for DSC measurements were prepared in the same manner as for the CD measurements described above. DSC measurements were performed on a MicroCal MCS (Northampton, MA), which was calibrated using pure paraffin hydrocarbons sealed in a steel capillary tube with an internal heater for calibration pulse. Both sample and reference cells were cleaned with 100 mL of weak alkaline solution (20 mM Tris, 10 mM EDTA, 5% SDS, pH 8.5) and rinsed with ethanol and distilled water. Measurement conditions were 0.5 K/min heating or cooling rate, 20 s filter period, and 300 s prescan wait period. To obtain maximum accuracy, we minimized the effects that arise from thermal history by overnight dummy scans before each measurement.

Basic thermodynamic parameters characteristic of the melting transition were obtained as outlined by Privalov (*28*). Heat capacities were further analyzed by the double deconvolution procedure (*29*) and nonlinear least-squares fitting method (*30*) using the program of SALS (*31*) or SigmaPlot (Jandel Scientific Software, San Rafael, CA).

Theoretical Basis for Unimolecular and Bimolecular Reactions. To accomplish thermodynamic analyses of the reconstituted and uncleaved domains, several fundamental equations for a general unimolecular reaction (A ⇌ B) and a bimolecular reaction ($\alpha\beta \rightleftharpoons \alpha + \beta$) were introduced. Allowing K and f to be the equilibrium constant and the fraction of unfolded and/or dissociated molecules, the relations between them are shown by eq 1 for the unimolecular reaction and by eq 2 for the bimolecular reaction:

[1] Abbreviations: PGB1, immunoglobulin G-binding domain B1 of streptococcal Protein G; DSC, differential scanning calorimetry; CD, circular dichroism; Fmoc, fluorenylmethoxycarbonyl; DMG, β,β'-dimethylglutaric acid; T_m, transition temperature; ΔH_m, change in enthalpy at transition temperature; ΔG_m, change in Gibbs free energy at transition temperature; ΔC_p, change in heat capacity from folded to unfolded state; NOESY, two-dimensional nuclear Overhauser enhancement and exchange spectroscopy; ASA, accessible surface area.

$$K_{uni} = \frac{[B]}{[A]}, \quad f_{uni} = \frac{[B]}{[A] + [B]}$$

$$\therefore K_{uni} = \frac{f_{uni}}{(1 - f_{uni})} \tag{1}$$

$$K_{bi} = \frac{[\alpha][\beta]}{[\alpha\beta]}, \quad f_{bi,\alpha} = \frac{[\alpha]}{[\alpha\beta] + [\alpha]} = \frac{[\alpha]}{C_{t,\alpha}},$$

$$f_{bi,\beta} = \frac{[\beta]}{[\alpha\beta] + [\beta]} = \frac{[\beta]}{C_{t,\beta}}$$

$$\therefore K_{bi} = \frac{f_{bi,\alpha} f_{bi,\beta}}{(1 - f_{bi,\alpha})} C_{t,\beta} = \frac{f_{bi,\alpha} f_{bi,\beta}}{(1 - f_{bi,\beta})} C_{t,\alpha} \tag{2}$$

where $C_{t,\alpha}$ and $C_{t,\beta}$ indicate total concentrations of each component in the bimolecular reaction. Provided that the two components were dissolved at equimolar concentration ($C_{t,\alpha} = C_{t,\beta}$), eq 2 can be simplified to

$$K_{bi} = \frac{{f_{bi}}^2}{(1 - f_{bi})} C_t \tag{3}$$

The equilibrium constants for the unimolecular and bimolecular reactions are also expressed by the van't Hoff equation, respectively:

$$K_{uni} = \exp\left\{ -\frac{\Delta H_m}{RT}\left(1 - \frac{T}{T_m}\right) - \frac{\Delta C_p}{RT}\left(T - T_m - T \ln\left(\frac{T}{T_m}\right)\right)\right\} \tag{4}$$

$$K_{bi} = \frac{C_t}{2} \exp\left\{ -\frac{\Delta H_m}{RT}\left(1 - \frac{T}{T_m}\right) - \frac{\Delta C_p}{RT}\left(T - T_m - T \ln\left(\frac{T}{T_m}\right)\right)\right\} \tag{5}$$

where ΔH_m and ΔC_p are the changes in enthalpy and in heat capacity, respectively, from the folded to the unfolded state at a transition temperature T_m.

Since heat capacity C_p is defined as differentials of enthalpy, the excess molar heat capacities C_p of both reactions are obtained as follows:

$$C_p = \frac{dH}{dT} = \frac{d}{dT}(H_F + \Delta H f) = \frac{dH_F}{dT} + \frac{d\Delta H}{dT} f + \Delta H \frac{df}{dT} \tag{6}$$

$$C_{p,uni} = C_{p,F} + \Delta C_p f_{uni} + \frac{(\Delta H_m + \Delta C_p (T - T_m))^2}{RT^2} f_{uni}(1 - f_{uni}) \tag{7}$$

$$C_{p,bi} = C_{p,F} + \Delta C_p f_{bi} + \frac{(\Delta H_m + \Delta C_p (T - T_m))^2}{RT^2} f_{bi}\left(\frac{1 - f_{bi}}{2 - f_{bi}}\right) \tag{8}$$

where $C_{p,F}$ is the molar heat capacity of components in folded state. Therefore, C_p can be fully described as the function of T with the parameters ΔC_p, ΔH_m, and T_m by substituting eqs 1 and 4 for eq 7, or eqs 3 and 5 for eq 8.

Similarly, the molecular ellipticities $[\theta]$ of both reactions are introduced from eq 9 and fully described as a function of T with the parameters ΔC_p, ΔH_m and T_m, by substituting eq 4 for eq 10, or eq 5 for eq 11:

$$[\theta] = [\theta]_F + ([\theta]_U - [\theta]_F) f \tag{9}$$

$$[\theta]_{uni} = [\theta]_F + ([\theta]_U - [\theta]_F) \frac{K_{uni}}{K_{uni} + 1} \tag{10}$$

$$[\theta]_{bi} = [\theta]_F + ([\theta]_U - [\theta]_F) \frac{-K_{bi} + \sqrt{{K_{bi}}^2 + 4 C_t K_{bi}}}{2 C_t} \tag{11}$$

where $[\theta]_F$ and $[\theta]_U$ are the molecular ellipticities of the component in the folded and unfolded states, respectively.

Thermodynamic Model for the Folding/Unfolding Equilibrium of the Reconstituted Domain. Since the C-terminal short fragment of PGB1(41−56) has been investigated to fold spontaneously into a nativelike β-hairpin structure at low temperature (*18, 19*), there should be four components at least in the equilibrium of thermal unfolding of the reconstituted domain. Thus, we need to develop more complicated equations than those used for a normal bimolecular reaction.

The folding/unfolding equilibrium of the reconstituted domain can be represented by the following reactions:

$$NC \overset{K_1}{\rightleftharpoons} N + C_F$$

$$C_F \overset{K_2}{\rightleftharpoons} C_U$$

where N, C_F, C_U, and NC indicate PGB1(1−40), PGB1(41−56) in β-hairpin structure, unfolded PGB1(41−56), and the associated complex PGB1(1−40)/PGB1(41−56). K_1 and K_2 are equilibrium constants for each reaction, defined by:

$$K_1 = \frac{[N][C_F]}{[NC]} = \frac{1}{(K_2 + 1)} \frac{f^2}{(1 - f)} C_t$$

$$K_2 = \frac{[C_U]}{[C_F]}$$

then,

$$f = \frac{[N]}{C_t}, \quad C_t = [NC] + [N] = [NC] + [C_F] + [C_U]$$

From these equations the dissociation constant for the reconstituted domain K_{rec} is also defined by:

$$K_{rec} = \frac{[N][C]}{[NC]} = \frac{[N]([C_F] + [C_U])}{[NC]} = K_1(K_2 + 1) \tag{12}$$

Therefore, the excess molar heat capacity C_p and the molecular ellipticity $[\theta]$ for the equilibrium of the reconstituted domain are as follows:

$$C_p = \frac{dH}{dT} = \frac{d}{dT}\left(H_{NC} + \left(\Delta H_1 + \frac{K_2}{K_2+1}\Delta H_2\right)f\right)$$
$$= \frac{dH_{NC}}{dT} + f\frac{d}{dT}\left(\Delta H_1 + \frac{K_2}{K_2+1}\Delta H_2\right) + \left(\Delta H_1 + \frac{K_2}{K_2+1}\Delta H_2\right)\frac{df}{dT}$$
$$= C_{p,NC} + \left(\Delta C_{p,1} + \frac{K_2}{K_2+1}\Delta C_{p,2}\right)f + \frac{1}{RT^2}\left(\Delta H_1 + \frac{K_2}{K_2+1}\Delta H_2\right)^2 f\left(\frac{1-f}{2-f}\right) + \frac{1}{K_2 RT^2}\left(\frac{K_2}{K_2+1}\Delta H_2\right)^2 f \quad (13)$$

$$[\theta] = [\theta]_{NC} + \left([\theta]_N + \frac{1}{K_2+1}[\theta]_{C_F} + \frac{K_2}{K_2+1}[\theta]_{C_U} - [\theta]_{NC}\right)f \quad (14)$$

where

$$f = \frac{-K_1(K_2+1) + \sqrt{K_1^2(K_2+1)^2 + 4C_tK_1(K_2+1)}}{2C_t} \quad (15)$$

$$K_1 = \frac{C_t}{2(K_2+1)}\exp\left\{-\frac{\Delta H_{m,1}}{RT}\left(1 - \frac{T}{T_{m,1}}\right) - \frac{\Delta C_{p,1}}{RT}\left(T - T_{m,1} - T\ln\left(\frac{T}{T_{m,1}}\right)\right)\right\} \quad (16)$$

$$K_2 = \exp\left\{-\frac{\Delta H_{m,2}}{RT}\left(1 - \frac{T}{T_{m,2}}\right) - \frac{\Delta C_{p,2}}{RT}\left(T - T_{m,2} - T\ln\left(\frac{T}{T_{m,2}}\right)\right)\right\} \quad (17)$$

$$\Delta H_1 = \Delta H_{m,1} + \Delta C_{p,1}(T - T_{m,1}) \quad (18)$$

$$\Delta H_2 = \Delta H_{m,2} + \Delta C_{p,2}(T - T_{m,2}) \quad (19)$$

Structure-Based Estimation of Thermodynamic Properties. Structure-based estimations of thermodynamic properties were performed from the values of the accessible surface area (ASA) of the domains and the empirical parameters of Makhatadze and Privalov (*32*). ASA was calculated by ProStat/Access_Surf option of Insight97 (Molecular Simulations Inc, Waltham, MA) using a probe with a radius of 1.4 Å and employing the algorithm of Shrake and Rupley (*33*) and van der Waals radii of Chothia (*34*). The coordinate of the folded structure of the uncleaved domain was taken from the entry code of 1pga (*11*) of the Brookhaven Protein Data Bank (*35*). ASA in the unfolded state was calculated by the same manner from the coordinate of the extended conformation ($\phi = -75°$, $\varphi = 180°$ for Pro and $\phi = 180°$, $\varphi = 180°$ for other 19 residues), which was generated by sequence builder of Quanta97 (Molecular Simulations Inc, Waltham, MA). Hydrogen atoms were neglected in all ASA calculations.

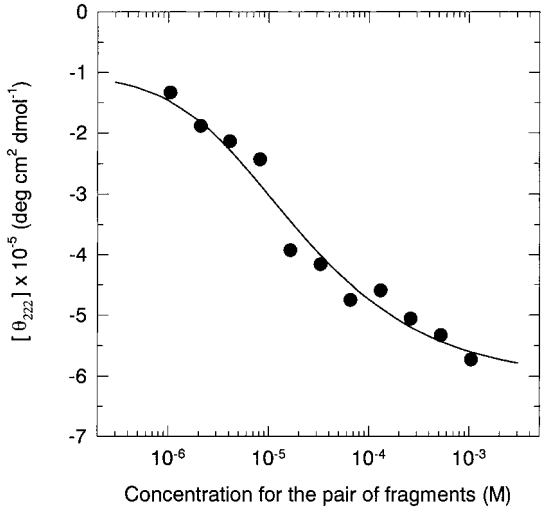

FIGURE 1: Association of the complementary fragments PGB1-(1−40) and PGB1(41−56) evaluated by molecular ellipticity at 222 nm. Equimolar concentrations of the fragments were dissolved in 50 mM phosphate buffer (pH 5.5) at 298 K. The closed circles and solid line show observed data and best fitted curve using eq 11, respectively.

RESULTS

Reconstitution from the Complementary Fragments. An equimolar mixing of the fragments PGB1(1−40) and PGB1-(41−56) in aqueous buffer solution led to spontaneous association between the two fragments followed by a significant conformational change, including an α-helix formation located at the mid-region of the molecule (*23*). Then, we estimated the degree of association by monitoring α-helix formation. Figure 1 shows the molecular ellipticity at 222 nm for solutions of equimolar fragments at 298 K, depending on the initial peptide concentration. By fitting eq 11 to the observed data with nonlinear least-squares methods, we determined the apparent dissociation constant of the reconstituted domain at this temperature ($K_{app} = 9 \times 10^{-6}$ M).

Reversible Transition in the Thermal Denaturation of the Reconstituted Domain. The secondary structure of the reconstituted domain monitored by CD at 222 nm was disrupted by a continuous heating at a fixed rate of 0.5 K/min (opened circles in Figure 2). Although this transition was quite broad (from 280 to 340 K), the sigmoid-shaped curve is typical of the thermal denaturation of ordinary globular proteins. This result indicates that the interaction between the two fragments is strong enough to generate a cooperative structure.

The disrupted structure was returned to its original conformation on cooling. Molecular ellipticity at 222 nm (closed circles in Figure 2) obtained from a continuous cooling measurement of the denatured sample at a fixed rate of 0.5 K/min was superimposable with that from the heating measurement. The results indicate that the thermal transition of the reconstituted domain is reversible and can be handled as a quasi-static process under the condition of a 0.5 K/min heating or cooling rate.

Folding/Unfolding Equilibrium of C-Terminal Short Fragment. The C-terminal short fragment PGB1(41−56) has been shown to fold spontaneously into a nativelike *β*-hairpin structure at low temperature (*18, 19*), whereas the N-terminal fragment PGB1(1−40) has a complete disordered structure

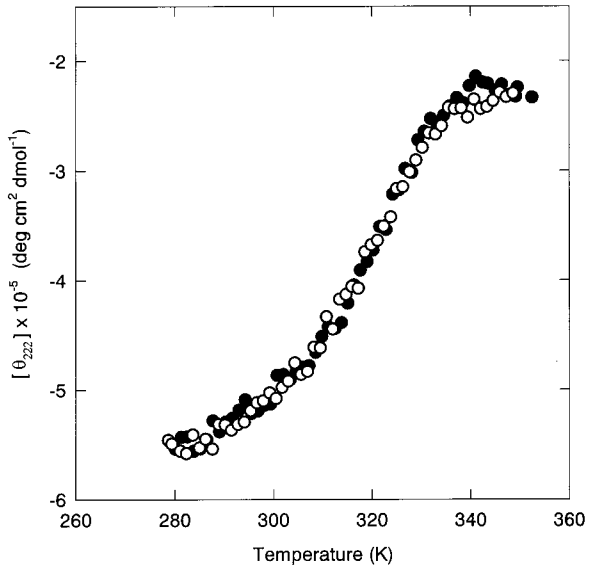

FIGURE 2: Temperature dependence of molecular ellipticity at 222 nm of the reconstituted domain, PGB1(1−40) + PGB1(41−56), in continuous heating (open circles) and in continuous cooling (closed circles) measurements. The sample was dissolved at 1.53 mM in 50 mM phosphate buffer (pH 5.4), and the heating/cooling rate was fixed at 0.5 K/min.

under aqueous conditions. Therefore, prior to the analysis of the reconstituted domain, the thermodynamic properties of PGB1(41−56) were determined first. Figure 3a shows the CD spectra of PGB1(41−56) at 275 and 343 K. Since the characteristic positive peak around 230 nm at 275 K indicates β-turn (*36*), which is a part β-hairpin structure, CD melting measurement at 230 nm was carried out to obtain the parameters for the thermal unfolding of PGB1(41−56). The β-hairpin structure of PGB1(41−56) was stabilized with minimal noncovalent interactions so that the curve obtained (thick line in Figure 3b) was very broad and did not cover the whole transition range. The fitted results, however, based on a typical two-state model using eq 10, were in reasonable agreement with the fluorescence study of [dansylated-Lys[57]]-PGB1(41−56) (*37*). Thermodynamic parameters for the unfolding of PGB1(41−56) were determined to be ΔH_m = 20.4 kJ mol^{-1}, T_m = 301.5 K, ΔS_m = 67.7 J K^{-1} mol^{-1}, and ΔC_p = 0.0 kJ K^{-1} mol^{-1}.

DSC Measurements of the Reconstituted and the Uncleaved Domains. Figure 4 shows the original output from calorimetry in the heating measurement of the reconstituted domain. The endothermic peak of the reconstituted domain was not large enough to neglect the instrumental error of intrinsic baseline repeatability (25 μcal/K). Then, we measured several buffer scans before and after each sample scan and subtracted them from the sample data, respectively. Subtracted data were analyzed individually, and the differences between the results were represented as the experimental error.

The theoretical curve (eq 13) was fitted to the experimental data of the reconstituted domain by nonlinear least-squares programs with varying adjustable parameters $T_{m,1}$, $\Delta H_{m,1}$, and $\Delta C_{p,1}$. In the calculation, the parameters $T_{m,2}$, $\Delta H_{m,2}$, and $\Delta C_{p,2}$ were fixed to the values which have been already determined by CD melting measurements of PGB1(41−56) as described above. The fitted curve (Figure 5, left) is nearly superimposable on the experimental data, indicating that the equilibrium thermodynamic model introduced in this study is reasonable for characterizing the folding energetics of the reconstituted domain. DSC curves of the uncleaved domain were also measured and fitted in the same manner, assuming a simple two-state model using eq 7 (Figure 4, right). All parameters obtained in this study are summarized in Table 1. The DSC data for the Met replacement mutant, [Met[1]]-PGB1(1−56), obtained by Alexander et al. (*12*) using a conductive type calorimeter are also listed. Although there are some methodological differences between Alexander's work and ours, especially for molecular coefficients for determining sample concentration (ϵ_{280} = 8180 vs 9530)[2] and the analytical procedures for determining ΔC_p (indirect method vs direct observation), the parameters in Table 1 are reasonable. Compared to the uncleaved domain, the reconstituted domain showed a broad peak shifted to lower temperature (by >40°). Because the curve was broad, the value of $\Delta C_{p,1}$ was not determined precisely in each experiment (ranging from 2.1 to 3.2 kJ K^{-1} mol^{-1}), but the mean value of this parameter was comparable with the value of the uncleaved wild-type domain. This agreement suggests that the reconstituted domain exposes almost the same hydrophobic area as wild-type upon thermal unfolding and that the solvent accessibilities of the reconstituted domain in the folded and unfolded states are similar to those of the uncleaved domain, respectively.

CD Melting Measurements of the Reconstituted Domain. To compare with the DSC results, several CD melting measurements of the reconstituted domain were also performed. The experimental data was analyzed by the same procedures using eq 14. The parameters shown in Table 1 are in reasonable agreement with the DSC measurements, indicating that the disruption of a single α-helix located in PGB1(1−40) occurs synchronously with the unfolding of the whole complex.

DISCUSSION

Our results for the reconstituted domain showed a thermal denaturation curve typical of ordinary globular proteins (Figures 2 and 4), noteworthy because the cleavage of a small single-domain protein is generally thought to lead to serious destabilization. In fact only a limited number of proteins that have been reconstituted from cleaved fragments have been reported. A classical example is the S-peptide/S-protein pair, corresponding to the residues 1−20 and 21−124 of ribonuclease S, respectively (*38*−*40*). The pairs of staphylococcal nuclease (6−48)/(49−149), (1−126)/(49−149), (1−126)/(111−149), barnase (1−102)/(88−110), (1−36)/(37−110), adenylate kinase (1−76)/(77−214), *trp* repressor (8−71)/(72−108), cytochrome *c* (1−38)/(87−104), chymotrypsin inhibitor-2 (20−59)/(60−83) and thioredoxin (1−73)/(74−108) have also been shown to have specific interactions (*41*−*48*). However, most pairs are greater than 10 kD and some of them consist of multiple domains. Furthermore, the mixing

[2] To determine the concentration, Alexander and co-workers used the value of 1.32 as the UV absorbance at 280 nm for a 1 mg/mL sample (*12*). The molecular weight of [Met[1]]PGB1 is calculated to be 6196.8 so that Alexander's coefficient corresponds to 8180 for a 1 M sample. By contrast, we used the value of 9530 for PGB1 in this work, which has been calculated from the standard values of aromatic amino acid residues (see text).

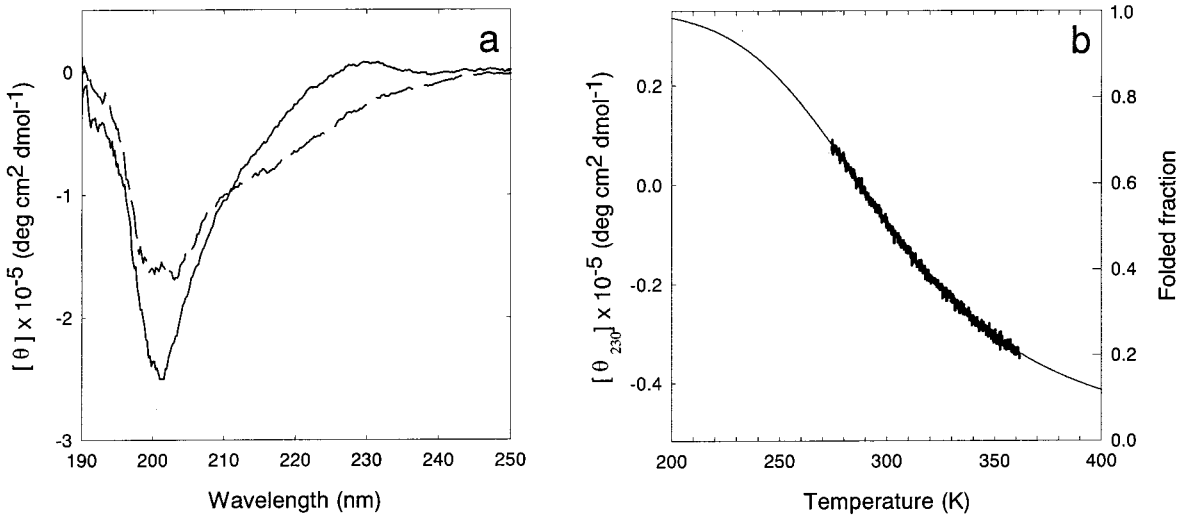

FIGURE 3: Folding/unfolding equilibrium of β-hairpin structure PGB1(41−56): (a) CD spectra of PGB1(41−56) in 50 mM phosphate buffer (pH 7.0) at 275 K (solid line) and 343 K (dashed line); (b) folded fraction of β-hairpin structure of PGB1(41−56) (thin line) calculated by nonlinear least-squares method. A typical two-state model (eq 10) was used to fit the result of the CD melting experiment (thick line) monitored at 230 nm at a constant heating rate 0.5 K/min from 275 to 363 K.

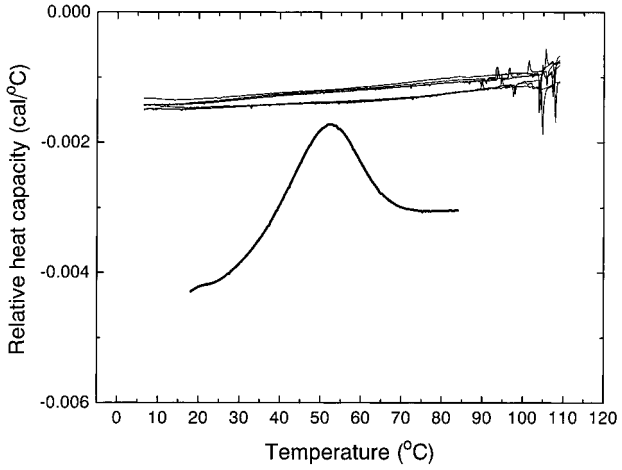

FIGURE 4: Typical data of DSC measurements. Thick and thin lines represent a sample scan of the reconstituted domain and buffer scans before and after the measurement, respectively.

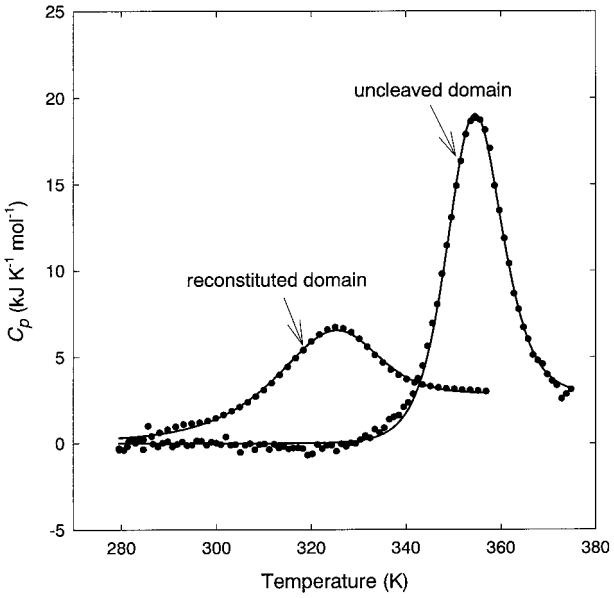

FIGURE 5: Thermal transition of the reconstituted (left) and the uncleaved (right) domains. Closed circles indicate DSC experimental data at a heating rate of 0.5 K/min. Sample concentrations were 1.42 and 0.82 mM, respectively, in 100 mM DMG buffer solution (pH 4.9 and 6.0) for the reconstituted and the uncleaved domains. Solid lines show theoretical curves best fitted by a nonlinear least-squares method (see text in detail).

of these pairs often results in only partial regeneration of the original activity or spectrum. Therefore, to our knowledge, PGB1(1−40) and PGB1(41−56) are the smallest fragment pair to have been successfully reconstituted.

Stability of the Reconstituted Domain. To characterize the thermodynamics of the association of the fragments, we first determined the values of the heat capacity, enthalpy, entropy, and Gibbs free energy changes from the folded state (NC) to the fully unfolded state (N + C_U) at standard state conditions (298 K, 1 M). The values calculated from the parameters of CD melting measurement at pH 4.9 (Table 1) were ΔC_p = 2.9 kJ K^{-1} mol^{-1}, ΔH =119 kJ mol^{-1}, ΔS = 307 J K^{-1} mol^{-1}, and ΔG = 28.1 kJ mol^{-1}. Positive values of ΔH and ΔS obviously indicate that the association was driven by enthalpy and entropically unfavorable. Compared to other protein−protein binding systems (*49*), ΔC_p, ΔH, and ΔS of the reconstituted domain are larger than average ($\Delta C_{p,avg}$ = 1.4 ± 0.86 kJ K^{-1} mol^{-1}, ΔH_{avg} = 36 ± 57 kJ mol^{-1}, and ΔS_{avg} = −26 ± 183 J K^{-1} mol^{-1}), while ΔG is smaller (ΔG_{avg} = 44 ± 10 kJ mol^{-1}). The reason for the large values of ΔC_p and ΔH is discussed in a later section. The small value of ΔG of the reconstituted domain is almost equal to that of subtilisin inhibitor-chymotrypsin system (30 kJ mol^{-1}) or cytochrome *c* peroxidase-cytochrome *c* system (29 kJ mol^{-1}), one of weakest complexes of 43 protein−protein binding systems summarized by Stites (*49*). Small ΔG is reflected in the fractions of free (unbound) fragments. We calculated the temperature dependence of the concentrations of the four components at equilibrium on the supposition that PGB1(1−40) and PGB1(41−56) were initially dissolved at 1.0 mM each (Figure 6). The figure shows that the fractions of the free fragments occupy 15% of total concentration at 298 K, and even at 273 K the fractions are not negligible. This explains the gradual increases of heat capacity and molar ellipticity at a low-temperature range observed in DSC and CD melting measurements (Figures 2 and 4).

Table 1: Thermodynamic Parameters for the Reconstituted Domain Consisting of PGB1(1−40) and PGB1(41−56) and That for the Uncleaved Wild Domain PGB1(1−56)

proteins	method	pH	conc (mM)	$T_{m,1}$ (K)	$\Delta H_{m,1}$ (kJ/mol)	$\Delta C_{p,1}$ (kJ K^{-1}mol^{-1})	$T_{m,2}$ (K)	$\Delta H_{m,2}$ (kJ/mol)	$\Delta C_{p,2}$ (kJ K^{-1}mol^{-1})
reconstituted domain	DSC	4.9	1.42	315 ± 0.8	114 ± 5	3.2 ± 0.3	301	20.4	0
PGB1(1−40)		5.9	0.78	313 ± 0.9	131 ± 5	2.1 ± 0.4	301	20.4	0
+	CD melting	4.9	1.42	319	161	2.9	301	20.4	0
PGB1(41−56)		5.9	0.82	315	150	2.8	301	20.4	0
		7.0	0.97	314	119	2.6	301	20.4	0
uncleaved domain									
PGB1(1−56)	DSC	6.0	0.82	354 ± 0.1	270 ± 0.5	2.7 ± 0.3			
[Met^1]PGB1(1−56)[a]	DSC	5.4		361	253	2.9			

[a] Data for Met replacement mutant were taken from Alexander (*12*).

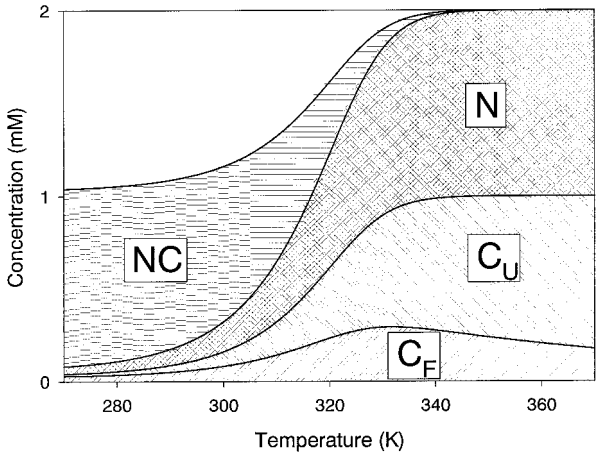

FIGURE 6: Concentrations of each component in the folding/unfolding equilibrium of the reconstituted domain. The values were calculated by eqs 15−19 and the parameters in Table 1 on the assumption that PGB1(1−40) and PGB1(41−56) were initially dissolved at 1.0 mM each. See text for the abbreviation of the components.

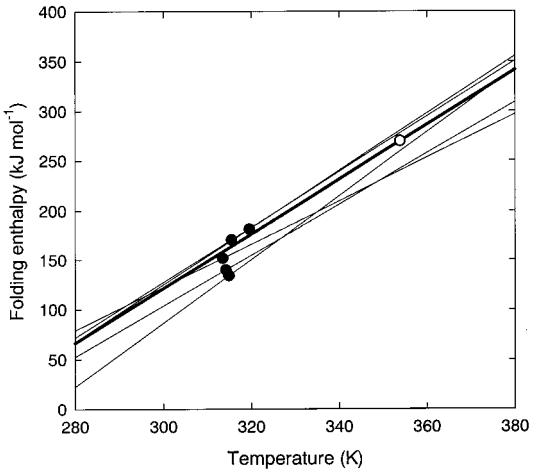

FIGURE 7: Temperature dependence of the change in enthalpy from the folded to the unfolded state, $\Delta H(T)$. The thin lines, the reconstituted domain, were calculated by

$$\Delta H(T) = \Delta H_1 + \Delta H_2 = \Delta H_{m,1} + \Delta C_{p,1}(T - T_{m,1}) + \Delta H_{m,2} + \Delta C_{p,2}(T - T_{m,2})$$

using the parameters in Table 1. The thick line, the uncleaved domain, was by

$$\Delta H(T) = \Delta H_m + \Delta C_p(T - T_m)$$

Closed and opened circles indicate ΔH_m of the reconstituted and the uncleaved domains, respectively.

Folding Enthalpy of the Reconstituted and Uncleaved Domains. For further evaluation of stability we should compare the reconstituted domain to the uncleaved domain using reasonable procedures. In many cases, stabilizing/destabilizing effects caused by mutations are represented quantitatively as a value of $\Delta\Delta G$. In this case, however, the value of ΔG is inadequate to compare the stability because the folding/unfolding equilibrium of the reconstituted domain is fundamentally a bimolecular reaction, whereas the uncleaved one is unimolecular. It is known that the value of ΔG in bimolecular reactions was not constant but variable, depending on definition of standard state (e.g., 1 mM instead of 1 M). Therefore we compared the values of ΔH, which is independent of the fragment concentration in both reactions, to evaluate the stability of the reconstituted domain. In Figure 7 the thin and thick lines show the temperature dependence of the enthalpy changes, $\Delta H(T)$, of the reconstituted and uncleaved domains, respectively. Most of the thin lines of the reconstituted domain, calculated from the set of parameters in Table 1, were almost superimposable to the thick line for the uncleaved domain. The averaged values of $\Delta H(T)$ for the reconstituted domain were close to that of the uncleaved domain, differing by less than 10 kJ mol^{-1} at any given temperature. This result indicates that the two fragments in the reconstituted domain, PGB1(1−40) and PGB1(41−56), associate each other with sufficient interactions to assume that the domain folds into the same structure as that of the wild-type domain. It also indicates that the various intramolecular noncovalent bonds that stabilize the native structure, such as hydrophobic interactions and hydrogen bonds, are regenerated to the same extent in the reconstituted domain.

In our previous paper (*23*), we investigated the resemblance of the secondary structures between the reconstituted and the uncleaved domains, deduced from the comparable CD spectra in far-UV region and the similar chemical shifts of α protons in 1D-NMR. Additionally, we investigated the similarity of parts of the tertiary structures, deduced from similar 2D-NMR spectra in the region from Thr^{44} to Lys^{50}. However, we did not determine the complete complex structure at atomic resolution, leaving the quantitative degree of reconstitution unclear. In other words, the previous results could be interpreted with various explanations for the physicochemical properties of the reconstituted domain. For example, a loosely condensed and partially folded complex or an entirely folded complex by induced-fit associations is a possible hypothesis. The former hypothesis is sometimes used to explain globular proteins in a molten globule (MG)

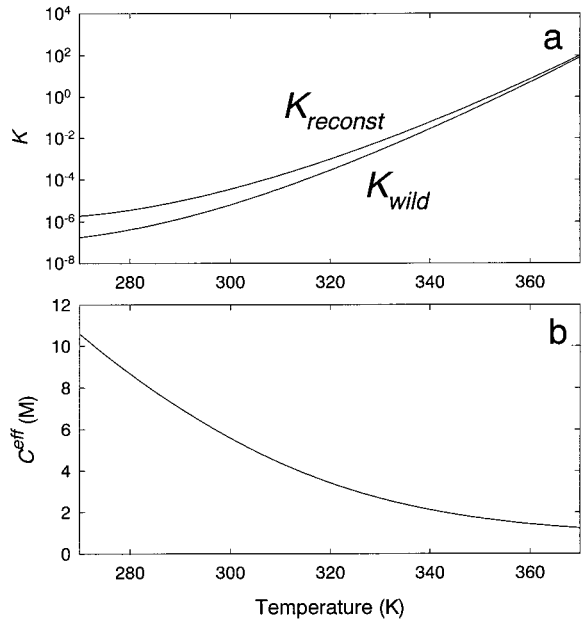

FIGURE 8: Concentration effect on the stability of the reconstituted domain: (a) temperature dependence of the equilibrium constants; (b) temperature dependence of the effective concentration.

state (*50*), which is generally considered to be a kinetic intermediate of the protein folding process (*51*). The latter explanation is often observed in ordinary protein−protein binding systems, such as a pair of antibody-hapten or receptor-peptide hormones. Thermodynamic analysis has shown that the degree of reconstitution is almost perfect and that the physicochemical property of the reconstituted domain should be considered comparable to ordinary protein−protein binding systems rather than globular proteins in MG state.

Evaluation of the Entropic Effect Contributing to the Stability of the Reconstituted Domain. Respective values of $\Delta H(T)$ also indicate that the apparent instability of the reconstituted domain (>40° lower in T_m) is primarily attributed to entropic disadvantage of a bimolecular reaction. In other words, the intramolecular free energy between the segment (1−40) and (41−56) in the uncleaved domain is promoted by the covalent connection 40−41 as much as the magnitude of the entropic effect from the level of the intermolecular free energy between PGB1(1−40) and (41−56) in the reconstituted domain. Since the folding/unfolding equilibrium of the reconstituted domain is fundamentally a bimolecular reaction, T_m should differ depending on the concentration of solutes so that the apparent instability is also represented as a function of concentration. To compare the concentration-dependent stability of the reconstituted domain to the independent stability of the uncleaved domain, we used "effective concentration". Effective concentration, C^{eff}, is defined as the ratio of equilibrium constants and is often used to evaluate the entropic cooperativity of intramolecular interactions (*52*). C^{eff} for the uncleaved domain was calculated by substituting eqs 4, 12, 16, and 17 for eq 20.

$$C^{eff} = \frac{K_{inter}}{K_{intra}} = \frac{K_{rec}}{K_{wild}} \qquad (20)$$

As shown in Figure 8, K_{wild} and K_{rec} increased from 10^{-7} to 10^{2} with increasing temperature while the C^{eff} decreased from 10 to 1 M (approximately 6 M at 298 K). These C^{eff} values indicate that the interactions between segments (1−40) and (41−56) of the uncleaved domain can be considered equivalent to the interactions of the corresponding fragments in the reconstituted domain should concentrations be in the 1∼10 M range. Although knowledge of the effective concentration of "noncovalent" interactions is important for understanding the contribution of entropic cooperativity to protein stability (*52*), other than the "covalent" formation of several cyclic compounds, little research has been done. Whereas the effective concentration of cyclization of small organic compounds was in the range of 10^2 to 10^9 M (*53*, *54*), the values of disulfide bond formation of unfolded proteins were 1−70 mM (*55*, *56*). Our C^{eff} values of the uncleaved domain indicate that the flexibility at the hinge region 40−41 is much larger than the linking part of the small organic compounds but smaller than that of the random polypeptide.

Structure-Based Estimation of Thermodynamic Properties of the Reconstituted Domain. Since Kauzmann (*57*) proposed that the "hydrophobic effect" should provide a large driving force for the folding process of proteins, many investigations of the relationship between the stability and the structure of proteins have been carried out. Consequently, that there is a close correlation between the thermodynamic properties and the exposed solvent accessible surface areas during unfolding (ΔASA) is generally accepted (*58*−*61*). We recently have been able to estimate the thermodynamic properties from ΔASA with a considerable accuracy (*32*, *62*−*64*). Therefore, by estimating the thermodynamic properties from the values of ΔASA we can gain insights into the folding energetics of the reconstituted domain.

The values of the polar, aliphatic, and aromatic surfaces of ΔASA of the uncleaved domain were determined to be 1638, 2133, and 534 Å^2, respectively. From these values we then calculated the heat capacity, enthalpy, and free energy changes at 298 K using the empirical parameters of Makhatadze and Privalov (*32*): $\Delta C_p = 3.0$ kJ K^{-1} mol^{-1}, $\Delta H = 89 \pm 49$ kJ mol^{-1}, and $\Delta G = 18 \pm 68$ kJ mol^{-1}. These estimated values were in reasonable agreement with our measured data of the uncleaved domain, indicating the reliability of such a structure-based estimation. We also calculated the respective thermodynamic parameters of the reconstituted domain while assuming that the fragments fold to the same structure of corresponding segments as per the wild-type domain. The polar, aliphatic, and aromatic ΔASAs of PGB1(1−40) were 987, 1244, and 184 Å^2, while those of PGB1(41−56) were 303, 321, and 103 Å^2, respectively. From these values we obtained $\Delta C_p = 1.5$ kJ K^{-1} mol^{-1}, $\Delta H = 50 \pm 30$ kJ mol^{-1}, and $\Delta G = -111 \pm 54$ kJ mol^{-1} for PGB1(1−40) and $\Delta C_p = 0.4$ kJ K^{-1} mol^{-1}, $\Delta H = 16 \pm 9$ kJ mol^{-1}, and $\Delta G = -97 \pm 25$ kJ mol^{-1} for PGB1(41−56) at 298 K. The negative free energy of each fragment is consistent with the observation that the individual fragment has difficulty maintaining the same rigid structure as it exists in the wild-type domain. Subtracting the sum of the fragments' ΔASAs from the ΔASA of the uncleaved domain, the interface area between two fragments in the reconstituted domain can be calculated and divided to the polar, aliphatic, and aromatic areas: 349, 569, and 248 Å^2. Since these areas are buried within the interior of the domain, when two fragments begin an association, the dehydration from the areas surrounding the interface and the contacts between the

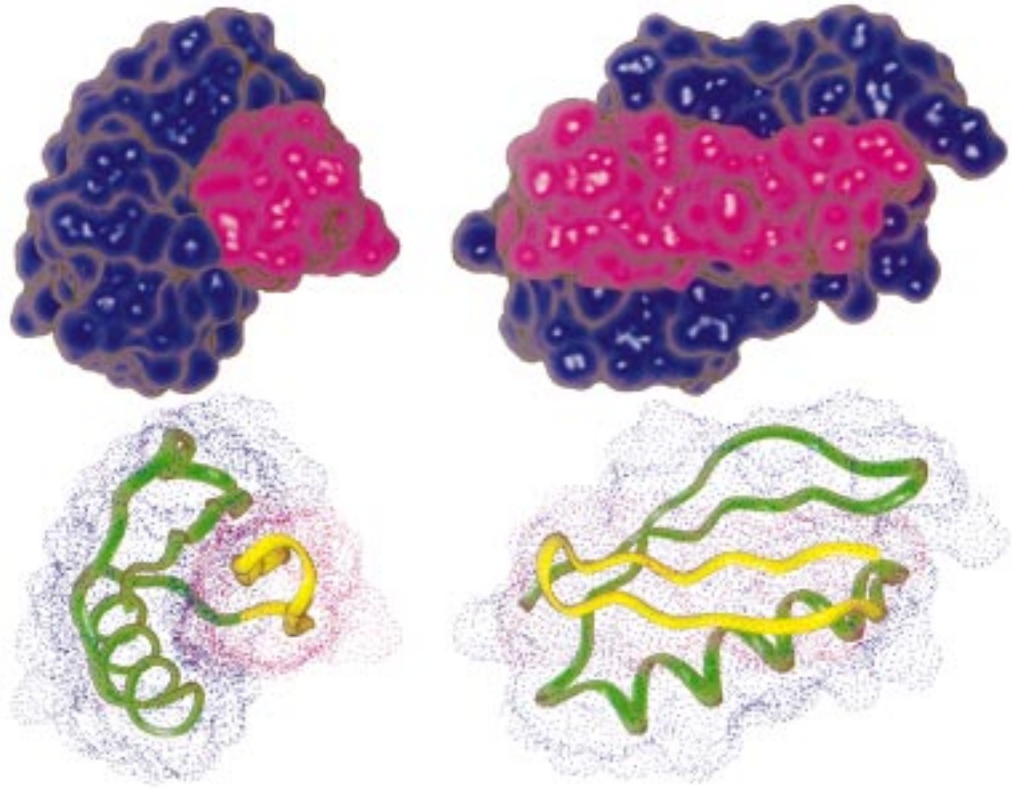

FIGURE 9: Schematic drawings of PGB1 from front and side views. In the surface model (top), the molecular surface (*70*) of segments (1−40) and (41−56) were respectively calculated with a probe radius of 1.4 Å and colored blue and red. In the ribbon model (bottom), the main chains of the segment (1−40) and (41−56) are shown as green and yellow, respectively. Their molecular surfaces are also represented by dots. All drawings were produced by the program Insight97 (Molecular Simulations Inc, Waltham, MA) using the coordinate data from PDB 1pga (*11*).

areas are essentially responsible for the intermolecular interaction between the fragments. The energy of the dehydration and the contact can be also estimated in the same manner: $\Delta C_p = 1.1$ kJ K^{-1} mol^{-1} and $\Delta H = 23 \pm 10$ kJ mol^{-1} at 298 K. These values are smaller than the observed data of the reconstituted domain, since the latter include internal interactions within each fragment. That is to say, the total (or observed) heat capacity and enthalpy changes are represented by two terms, as follows:

$$\Delta C_{p,obs} = \Delta C_{p,inter} + \Delta C_{p,intra} \quad (21)$$

$$\Delta H_{obs} = \Delta H_{inter} + \Delta H_{intra} \quad (22)$$

where the suffixes *inter* and *intra* represent the interchain and intrachain interactions, respectively. Structure-based estimation indicates that approximately 35% of the total heat capacity change and approximately 25% of the total enthalpy change can be attributed to interchain interaction between the fragments at 298 K. The average values of the 43 protein−protein binding systems described in the first section of the discussion are closer in value to the estimated interchain heat capacity and enthalpy changes than to the total values obtained in our experiment.

Implications to the Folding Mechanism of the Wild-Type Domain. In 1976, Karplus and Weaver discussed the dynamics of protein folding and proposed the diffusion−collision model as a possible mechanism (*22*). Since then, several different models have been proposed, such as the framework model (*65*), the clusters or embryos model (*66*), the nucleation−condensation model (*67*), and the foldon model (*68*). Although there were some differences among the models, the essential concept is common: a protein is composed of several kinetic components and folds hierarchically through the dynamic association between the components. In the diffusion−collision model, the component called microdomain (*22*), a fluctuating quasi-particle, folds quasi-independently. The microdomain moves diffusively while the collisions between them take place. Collisions can lead to coalescence into multi-microdomain intermediates, which may give rise to the entire folding process.

Analyzing the association of complementary fragments of a small protein is a powerful and important approach (*69*) to verify the models and investigate the folding mechanism experimentally. Unfortunately, the thermodynamics of the association of complementary fragments have hampered research, due to the low stability of the complex. Thus, our results for the reconstituted domain composed of two complementary fragments are noteworthy. The almost complete regeneration of the intramolecular noncovalent bonds in the reconstituted domain prove that the fragments possess the same potential to fold as the native domain, although the N-terminal fragment PGB1(1−40) is not able to fold individually into a stable and rigid structure. The apparent instability of the reconstituted domain compared to the uncleaved domain is primarily attributed to entropic disadvantage in a bimolecular reaction. These findings strongly indicate that the segments (1−40) and (41−56) act as a microdomain in the native folding. The values of the heat capacity and enthalpy changes of the intermolecular interaction between the two fragments estimated from the ΔASA

of the interface area were similar to the averaged values of ordinary protein−protein systems. The results imply that the associating driving force for organizing microdomains is not special but common. In previous work (*23*) we examined various pairs of fragments that differed by the point of cleavage along the sequence of PGB1 and found that only one pair, that is, PGB1(1−40) and (41−56), showed a specific interaction between the fragments. This supports the contention that only this pair of fragments, not other pairs, can be classified to a lower hierarchical level of the kinetical folding. The effective concentration analysis suggests that the collision between the microdomains, that is, segments (1−40) and (41−56), would take place at certain frequencies which are theoretically calculated from the virtual solution of approximately 6 M fragments at 298 K.

In the structure-based estimation, the C-terminal short fragment PGB1(41−56) is somewhat more stable than PGB1(1−40), suggesting the possibility that segment (41−56) folds prior to segment (1−40), thus acting as a nucleus in the folding process of the whole domain. This hypothesis is also supported by the discovery that a considerable amount of PGB1(41−56) folds into nativelike β-hairpin structure at low temperatures (*18*, *19*). By drawing the structure of the two segments separately (Figure 9), one notices that the side surface of the columnar-shaped segment (41−56) is surrounded by the surface of the segment (1−40). Moreover, the main chain of the segment (41−56) is grasped by the α-helix and β-sheet structures of the segment (1−40) like a hot dog. The structure allows us to envision that PGB1 folds through the kinetic organization of the segments.

ACKNOWLEDGMENT

We wish to express our gratitude to Dr. Shun-ich Kidokoro (Sagami Chemical Research Center) for his helpful suggestions for analysis of the thermodynamic data. Also Dr. Kunihiro Kuwajima (University of Tokyo) for valuable comments. The technical assistance of Mr. Hirofumi Yoshii (University of Tsukuba) for preparing peptide fragments is gratefully acknowledged.

REFERENCES

1. Levinthal, C. (1968) *J. Chim. Phys. 65*, 44−45.
2. Baldwin, R. L. (1994) *Nature 369*, 183−184.
3. Onuchic, J. N., Wolynes, P. G., Luthey-Schulten, Z., and Socci, N. D. (1995) *Proc. Natl. Acad. Sci. U.S.A 92*, 3626−3630.
4. Wolynes, P. G., Onuchic, J. N., and Thirumalai, D. (1995) *Science 267*, 1619−1620.
5. Dill, K. A., and Chan, H. S. (1997) *Nat. Struct. Biol. 4*, 10−19.
6. Gilbert, H. F. (1994) in *Mechanisms of Protein Folding* (Pain, R. H., Ed.) pp 104−136, Oxford University Press, Oxford, U.K.
7. Nall, B. T. (1994) in *Mechanisms of Protein Folding* (Pain, R. H., Ed.) pp 80−103, Oxford University Press, Oxford, U.K.
8. Garel, J.-R. (1992) in *Protein Folding* (Creighton, T. E., Ed.) pp 405−454, W. H. Freeman and Company, New York.
9. Gronenborn, A. M., Filpula, D. R., Essig, N. Z., Achari, A., Whitlow, M., Wingfield, P. T., and Clore, G. M. (1991) *Science 253*, 657−661.
10. Achari, A., Hale, S. P., Howard, A. J., Clore, G. M., Gronenborn, A. M., Hardman, K. D., and Whitlow, M. (1992) *Biochemistry 31*, 10449−10457.
11. Gallagher, T., Alexander, P., Bryan, P., and Gilliland, G. L. (1994) *Biochemistry 33*, 4721−4729.
12. Alexander, P., Fahnestock, S., Lee, T., Orban, J., and Bryan, P. (1992) *Biochemistry 31*, 3597−3603.
13. Orban, J., Alexander, P., and Bryan, P. (1994) *Biochemistry 33*, 5702−5710.
14. Orban, J., Alexander, P., Bryan, P., and Khare, D. (1995) *Biochemistry 34*, 15291−15300.
15. Alexander, P., Orban, J., and Bryan, P. (1992) *Biochemistry 31*, 7243−7248.
16. Kuszewski, J., Clore, G. M., and Gronenborn, A. M. (1994) *Protein Sci. 3*, 1945−1952.
17. Park, S. H., O'Neil, K. T., and Roder, H. (1997) *Biochemistry 36*, 14277−14283.
18. Kobayashi, N., Endo, S., and Munekata, E. (1993) *Pept. Chem. 1992*, 278−280.
19. Blanco, F. J., Rivas, G., and Serrano, L. (1994) *Nat. Struct. Biol. 1*, 584−590.
20. Blanco, F. J., Jimenez, M. A., Pineda, A., Rico, M., Santoro, J., and Nieto, J. L. (1994) *Biochemistry 33*, 6004−6014.
21. Blanco, F. J., and Serrano, L. (1995) *Eur. J. Biochem. 230*, 634−649.
22. Karplus, M., and Weaver, D. L. (1976) *Nature 260*, 404−406.
23. Kobayashi, N., Honda, S., Yoshii, H., Uedaira, H., and Munekata, E. (1995) *FEBS Lett. 366*, 99−103.
24. Gill, S. C., and von Hippel, P. H. (1989) *Anal. Biochem. 182*, 319−326.
25. Honda, S., Ohashi, S., Morii, H., and Uedaira, H. (1991) *Biopolymers 31*, 869−876.
26. Honda, S., Morii, H., Ohashi, S., and Uedaira, H. (1991) *Biochim. Biophys. Acta 1068*, 81−86.
27. Honda, S., Odahara, T., Uedaira, H., and Miyake, J. (1994) *Rep. Natl. Inst. Biosci. Hum.-Technol. (Jpn.) 2*, 17−20.
28. Privalov, P. L. (1979) *Adv. Protein Chem. 33*, 167−241.
29. Kidokoro, S., and Wada, A. (1987) *Biopolymers 26*, 213−229.
30. Kidokoro, S., Uedaira, H., and Wada, A. (1988) *Biopolymers 27*, 271−297.
31. Nakagawa, T., and Oyanagi, Y. (1980) in *Recent developments in statistical inference and data analysis* (Matusita, K., Ed.) pp 221−225, North-Holland Pub. Co.
32. Makhatadze, G. I., and Privalov, P. L. (1995) *Adv. Protein Chem. 47*, 307−425.
33. Shrake, A., and Rupley, J. A. (1973) *J. Mol. Biol. 79*, 351−371.
34. Chothia, C. (1975) *Nature 254*, 304−308.
35. Bernstein, F. C., Koetzle, T. F., Williams, G. J., Meyer, E. E., Jr., Brice, M. D., Rodgers, J. R., Kennard, O., Shimanouchi, T., and Tasumi, M. (1977) *J. Mol. Biol. 112*, 535−542.
36. Chang, C. T., Wu, C.-S. C., and Yang, T. J. (1978) *Anal. Biochem. 91*, 13−31.
37. Muñoz, V., Thompson, P. A., Hofrichter, J., and Eaton, W. A. (1997) *Nature 390*, 196−199.
38. Richards, F. M., and Vithayathil, P. J. (1959) *J. Biol. Chem. 234*, 1459−1465.
39. Kato, I., and Anfinsen, C. B. (1969) *J. Biol. Chem. 244*, 1004−1007.
40. Catanzano, F., Giancola, C., Graziano, G., and Barone, G. (1996) *Biochemistry 35*, 13378−13385.
41. Taniuchi, H., and Anfinsen, C. B. (1971) *J. Biol. Chem. 246*, 2291−2301.
42. Hartley, R. W. (1977) *J. Biol. Chem. 252*, 3252−3254.
43. Sancho, J., and Fersht, A. R. (1992) *J. Mol. Biol. 224*, 741−747.
44. Saint Girons, I., Gilles, A. M., Margarita, D., Michelson, S., Monnot, M., Fermandjian, S., Danchin, A., and Barzu, O. (1987) *J. Biol. Chem. 262*, 622−629.
45. Tasayco, M. L., and Carey, J. (1992) *Science 255*, 594−597.
46. Wu, L. C., Laub, P. B., Elove, G. A., Carey, J., and Roder, H. (1993) *Biochemistry 32*, 10271−10276.
47. de Prat Gay, G., and Fersht, A. R. (1994) *Biochemistry 33*, 7957−7963.
48. Tasayco, M. L., and Chao, K. (1995) *Proteins 22*, 41−44.
49. Stites, W. E. (1997) *Chem. Rev. 97*, 1233−1250.

50. Ohgushi, M., and Wada, A. (1983) *FEBS Lett. 164*, 21−24.
51. Christensen, H., and Pain, R. H. (1994) in *Mechanisms of Protein Folding* (Pain, R. H., Ed.) pp 55−79, Oxford University Press, Oxford, U.K.
52. Creighton, T. E. (1993) *Proteins: Structures and Molecular Properties*, 2nd ed., W. H. Freeman and Company, New York.
53. Kirby, A. J. (1980) *Adv. Phys. Org. Chem. 17*, 183−278.
54. Chau, M. H., and Nelson, J. W. (1991) *FEBS Lett. 291*, 296−298.
55. Goldenberg, D. P. (1985) *J. Cell Biochem. 29*, 321−335.
56. Creighton, T. E. (1992) in *Protein Folding* (Creighton, T. E., Ed.) pp 405−454, W. H. Freeman and Company, New York.
57. Kauzmann, W. (1959) *Adv. Protein Chem. 14*, 1−63.
58. Ooi, T., Oobatake, M., Nemethy, G., and Scheraga, H. A. (1987) *Proc. Natl. Acad. Sci. U.S.A 84*, 3086−3090.
59. Spolar, R. S., Ha, J. H., and Record, M. T., Jr. (1989) *Proc. Natl. Acad. Sci. U.S.A 86*, 8382−8385.
60. Privalov, P. L., and Makhatadze, G. I. (1990) *J. Mol. Biol. 213*, 385−391.
61. Murphy, K. P., and Gill, S. J. (1991) *J. Mol. Biol. 222*, 699−709.
62. Murphy, K. P., and Freire, E. (1992) *Adv. Protein Chem. 43*, 313−361.
63. Freire, E. (1993) *Arch. Biochem. Biophys. 303*, 181−184.
64. Oobatake, M., and Ooi, T. (1993) *Prog. Biophys. Mol. Biol. 59*, 237−284.
65. Kim, P. S., and Baldwin, R. L. (1982) *Annu. Rev. Biochem. 51*, 459−489.
66. Go, N. (1983) *Annu. Rev. Biophys. Bioeng. 12*, 183-210.
67. Itzhaki, L. S., Otzen, D. E., and Fersht, A. R. (1995) *J. Mol. Biol. 254*, 260−288.
68. Panchenko, A. R., Luthey-Schulten, Z., and Wolynes, P. G. (1996) *Proc. Natl. Acad. Sci. U.S.A 93*, 2008−2013.
69. de Prat-Gay, G. (1996) *Protein Eng. 9*, 843−847.
70. Richards, F. M. (1977) *Annu. Rev. Biophys. Bioeng. 6*, 151−176.

BI982271G